

Automated segmentation of blood-flow regions in large thoracic arteries using 3D-cine PC-MRI measurements

Roy van Pelt · Huy Nguyen · Bart ter Haar Romeny · Anna Vilanova

Received: 8 January 2011 / Accepted: 30 June 2011 / Published online: 21 July 2011
© CARS 2011

Abstract

Purpose Quantitative analysis of vascular blood flow, acquired by phase-contrast MRI, requires accurate segmentation of the vessel lumen. In clinical practice, 2D-cine velocity-encoded slices are inspected, and the lumen is segmented manually. However, segmentation of time-resolved volumetric blood-flow measurements is a tedious and time-consuming task requiring automation.

Methods Automated segmentation of large thoracic arteries, based solely on the 3D-cine phase-contrast MRI (PC-MRI) blood-flow data, was done. An active surface model, which is fast and topologically stable, was used. The active surface model requires an initial surface, approximating the desired segmentation. A method to generate this surface was developed based on a voxel-wise temporal maximum of blood-flow velocities. The active surface model balances forces, based on the surface structure and image features derived from the blood-flow data. The segmentation results were validated using volunteer studies, including time-resolved 3D and 2D blood-flow data. The segmented surface was intersected with a velocity-encoded PC-MRI slice, resulting in a cross-sectional contour of the lumen. These cross-sections were compared to reference contours that were manually delineated on high-resolution 2D-cine slices.

Results The automated approach closely approximates the manual blood-flow segmentations, with error distances on the order of the voxel size. The initial surface provides a close approximation of the desired luminal geometry. This improves the convergence time of the active surface and facilitates parametrization.

Conclusions An active surface approach for vessel lumen segmentation was developed, suitable for quantitative analysis of 3D-cine PC-MRI blood-flow data. As opposed to prior thresholding and level-set approaches, the active surface model is topologically stable. A method to generate an initial approximate surface was developed, and various features that influence the segmentation model were evaluated. The active surface segmentation results were shown to closely approximate manual segmentations.

Keywords Image segmentation · Active surface · Phase-contrast MRI · Blood flow

Introduction

Cardiovascular disease (CVD) is a class of conditions affecting the heart and blood vessels. At present, CVD has an estimated overall prevalence of over thirty percent of the American population [2] and is currently the leading cause of death worldwide.

Blood-flow mechanics play an important role in the progression of cardiovascular diseases. Flowing blood directly interacts with the cardiovascular biology, possibly altering its morphology. Pre-clinical research, therefore, aims to understand the complex dynamical behavior of the blood flow. New insights into the hemodynamic behavior may reveal relevant information for future diagnosis and prognosis.

In the past, experimental flow measurements and computational fluid dynamics (CFD) simulations provided the predominant source of information for analyzing the hemodynamic behavior. Nowadays, blood-flow velocities can also be measured by a wide range of imaging modalities, ruling out model assumptions. However, measurements come with acquisition artefacts and resolution deficiencies. In this work,

R. van Pelt (✉) · H. Nguyen · B. ter Haar Romeny · A. Vilanova
Eindhoven University of Technology, Den Dolech 2, 5612 AZ,
Eindhoven, The Netherlands
e-mail: r.f.p.v.pelt@tue.nl

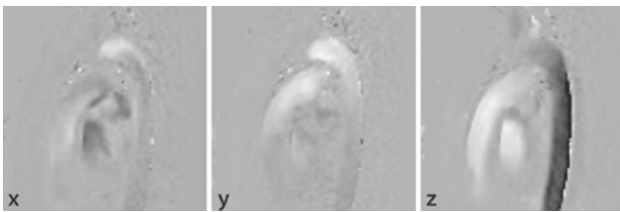


Fig. 1 A sagittal slice of 3D-cine PC-MRI blood-flow velocity data, depicted by the directions of acquisition at systole, where **x** conveys the flow in right-to-left direction, **y** in anterior-to-posterior direction and **z** in feet-to-head direction

we focus on blood-flow velocity information, acquired non-invasively by magnetic resonance imaging (MRI).

Phase-contrast MRI methods enable acquisition of time-resolved 3D blood-flow velocity fields, as depicted in Fig. 1. The resulting data is linearly related to the actual blood-flow velocities and can, therefore, be analyzed quantitatively. A typical data set encodes a full heartbeat, comprising 20–25 phases with a spatial resolution of $128 \times 128 \times 50$ voxels. The size of the voxels is generally on the order of two to three millimeters, and slightly anisotropic. A wide range of blood-flow characteristics can be derived from the acquired blood-flow velocities. For example, cardiac output, regurgitation fraction, and pressure can be computed.

Meaningful quantification of blood-flow characteristics requires accurate segmentation of the vessel lumen. In clinical practice, segmentations are typically obtained by manual delineation of the vessel circumference on a 2D slice, at one or more phases of the cardiac cycle. In case of velocity-encoded data, the blood-flow lumen may be delineated. Despite the intra- and inter-observer variability of these manual segmentations, this approach is sufficiently fast and accurate for practical purposes.

Extending the segmentation approach to a 3D-cine data set is non-trivial. While segmentation in a 2D-cine case comprising a single circumference, segmentation of volumetric data results in a 3D surface (Fig. 2).

Manual segmentation of 3D-cine blood-flow data is laborious and time-consuming and, therefore, not suitable for clinical practice. An automated segmentation approach is required, based on the 3D-cine PC-MRI blood-flow data.

On occasion, no high-quality anatomical data are available, next to the velocity-encoded data. For these cases, quantitative analysis should be possible as well. Therefore, our segmentation approach includes blood-flow data only. As a result, the segmentation cannot approximate the vessel wall morphology. Instead, the segmentation will distinguish the blood-flow regions from surrounding stationary tissues throughout the cardiac cycle, capturing the luminal geometry.

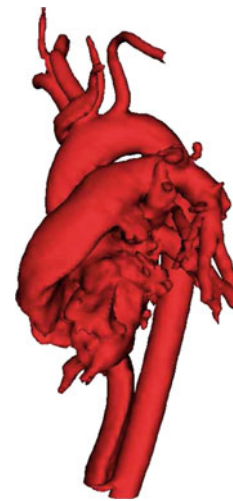


Fig. 2 Active surface segmentation of the PC-MRI-acquired cardiovascular blood-flow field

Background

Over the past two decades, a large body of research has focussed on the acquisition of MRI blood-flow velocity fields. In particular, 2D-cine blood-flow acquisition has become a mature modality, suitable for clinical practice. Consequently, 2D-cine blood-flow information is commonly acquired for complex conditions, such as congenital heart defects. In contrast, acquisition of 3D-cine PC-MRI blood-flow data is rather novel, and therefore, subject to further investigation and standardization.

In general, segmentation of the vessel lumen enables more accurate quantification of the inspected blood-flow parameters, as well as improved quality of visual representations. A wide range of studies investigate the behavior of pathological blood flow. Such analyses can rely on local inspection, using planar reformats or pathlines visualizations, as presented by Markl et al. [8,9]. In addition, segmentation can be performed locally, providing contours that intersect the vasculature at specified regions of interest [15].

Alternatively, the workflow may include a global segmentation step, using either anatomical images [9,13] or angiographic images [6]. It is possible to derive such angiographic images from the 3D-cine MRI blood-flow data.

In addition to morphological and angiographic information, the full blood-flow velocity information can be incorporated into the segmentation process, using both speed and direction information. This results in more accurate segmentation of the luminal geometry.

The amount of literature that specifically explores segmentations for blood-flow velocity fields is limited. Chung et al. [3] have segmented the vasculature in the brain, based on phase-contrast MRI blood-flow data. They employ the local coherence of the velocities, using a scalar-valued mea-

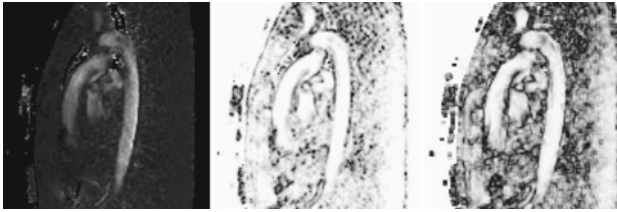


Fig. 3 Image feature intensities. Respectively blood-flow speed, local phase coherence and eigenvalue coherence. Within the blood-flow regions, intensities are high, with a discontinuity on the boundaries with stationary tissue

sure called the local phase coherence (LPC). The luminal geometry is segmented using automated thresholds on the histogram of coherence values. The LPC measure clearly indicates the boundaries of the vessel lumen. However, the presented thresholding approach is noise prone and relies on various assumptions concerning the histogram distribution.

In contrast, Solem et al. [12] and Persson et al. [11] have proposed a level-set segmentation, also using the blood-flow coherence. Their coherence measure, called the eigenvalue coherence (EVC), relies on local orientation distributions of the velocities. The blood flow is said to be locally coherent when a local distribution has one predominant orientation. This is determined by eigenanalysis of the average structure tensor. Although a level-set approach is versatile and robust, topological changes may cause the segmentation to structurally branch. This is undesirable when the structure of the luminal geometry is known a priori.

Furthermore, active shape [14] and active appearance models are widely used. These methods incorporate domain-specific knowledge, which often results in poor segmentations of anomalous morphologies.

In this work, we present a segmentation of the large thoracic arteries, based on 3D-cine PC-MRI blood-flow data. Instead of local 2D segmentations of the vasculature [9, 15], we present a global segmentation of the blood-flow lumen. Therefore, we employ an active surface model, as opposed to thresholding, level-set, or active shape approaches. An active surface benefits from topological stability, preventing undesirable branches, splits, or holes in the surface. Moreover, active surfaces are generally more accurate than thresholds and outperform level-sets in terms of computation time.

Our custom-made active surface model is based on the velocity information, including blood-flow direction through coherence measures found in literature. To the best of our knowledge, an active surface approach, based on full velocity information, has not been employed for segmentation of the blood-flow lumen before. In general, active surface models require an initial surface that approximates the final segmentation result. Therefore, we introduce a novel approach to extract the initial approximate surface from a temporal maximum volume of the

blood-flow speed intensities. We have validated our segmentation results against manual segmentations, performed on 2D-cine velocity-encoded PC-MRI slices with higher spatial resolution. This validation shows the performance of the various measures underlying the active surface model.

In summary, the main contributions of this paper are as follows:

- An active surface model for fast, accurate, and topologically stable segmentation of blood-flow regions within the large thoracic arteries. We introduce a novel approach to generate an approximate initial surface, based on a temporal maximum speed volume, and predict our potential forces upon different blood-flow coherence measures.
- A validation study, demonstrating the feasibility of active surface segmentation of the blood-flow lumen, and measuring the performance of various features against manual segmentation on 2D-cine velocity-encoded PC-MRI slices.

Methodology

We aim to distinguish blood-flow regions from stationary tissues. This distinction is based on the assumption that the speed of displacement of cardiovascular structures is substantially slower than the speed of flowing blood. This assumption is necessary because the MRI sequence encodes velocities of all tissues. In addition, we assume that flowing blood is locally coherent.

We have developed a custom active surface approach. Active surface models require an initial surface that roughly approximates the final segmentation. This initial surface will be attracted towards the desired boundaries of the blood-flow lumen, requiring forces based on image features. The image features are derived from the blood-flow data (Fig. 3). To segment the lumen, these features should emphasize the boundaries between blood-flow regions and stationary tissue.

Our segmentation methodology is structured as follows:

- Initial surface extraction (“Initial surface extraction”): First, we extract an initial surface, which will be subject to the forces imposed by the active surface model.
- Feature extraction (“Feature extraction”): Second, we pre-compute the image features, which will define an attractor image. An attractor image drives the potential forces of the active surface model.
- Active surface segmentation (“Active surface segmentation”): The active surface model performs an energy optimization to obtain the desired segmentation of the blood-flow

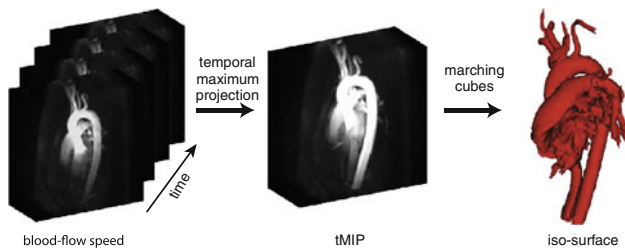


Fig. 4 A temporal maximum speed volume (tMSV) takes the maximum blood-flow speed for each voxel throughout the cardiac cycle. An initial surface can be extracted from this static representation of the blood-flow regions. A standard marching cubes algorithm is employed to generate the iso-surface

lumen, deforming the initial surface based on the attractor image and the surface shape.

Initial surface extraction

An active surface approach requires an initial approximate surface. Therefore, we present a novel approach to generate the initial surface, providing a good first approximation of the luminal geometry.

First, we derive a static representation of the temporal behavior of the blood flow. This pre-processing step results in a scalar-valued volume, called a temporal maximum speed volume (tMSV). This volume represents the peak blood-flow speed intensity over time and resembles an angiographic image, as depicted in Fig. 4. For each voxel, the maximum blood-flow speed throughout the cardiac cycle is selected from the velocity field $\vec{v}(\mathbf{x})$. Hence, the tMSV at each voxel position \mathbf{x} is defined for N cardiac phases as:

$$\text{tMSV}(\mathbf{x}) = \max (|\vec{v}(\mathbf{x})|_{i_i}) \quad \text{for } i = 0, \dots, N - 1 \quad (1)$$

Second, we generate the initial surface, using the tMSV volume. An iso-surface is extracted by roughly setting an iso-threshold. We aim for an initial approximate surface, and therefore, the iso-threshold can be determined visually. Variation of the iso-threshold will provide a different initial surface, but will not strongly affect the results of the active surface model. For the iso-surface extraction, we have employed the marching cubes algorithm [7] (see Fig. 4).

Feature extraction

In order to define attracting forces for the active surface model, we require features that emphasize the boundaries between blood-flow regions and stationary tissue. Therefore, the features should be sensitive to the blood-flow speed and direction, which means that the feature intensities should be unidirectionally affected as a function of the variations in the blood-flow velocities. In addition, we require that the features are spatially robust to noise.

Blood-flow speed (BFS)

The blood-flow speed is commonly inspected in angiograms and is employed by the majority of segmentation approaches. BFS is defined as the length of velocity \vec{v} at each voxel position \mathbf{x} :

$$\text{bfs}(\mathbf{x}) = \|\vec{v}(\mathbf{x})\| = \sqrt{\vec{v}(\mathbf{x})_x^2 + \vec{v}(\mathbf{x})_y^2 + \vec{v}(\mathbf{x})_z^2} \quad (2)$$

This feature is not sensitive to the blood-flow direction and is commonly computed without local averaging. Averaging the speed information in a local neighborhood improves noise-robustness, at the expense of contrast near the sought edges. Alternatively, the noise can be suppressed by masking the velocities with a complex-difference reconstruction of the original MRI data [10].

Local Phase Coherence (LPC)

Besides speed, also direction information provides valuable information for the segmentation process. Directions of the blood-flow field are said to be locally coherent, as opposed to blood-flow velocities near the boundaries.

Chung et al. [3] introduced the LPC metric, locally measuring the coherence as a scalar value for each voxel of the data set. They compute the *average angle* between a velocity vector and its direct neighbors. Thereto, they compute the sum of inner products of each unit-length velocity vector \hat{v} with the unit-length velocities of the direct neighbors. The result is normalized by the amount of velocities M in the neighborhood.

$$\text{lpc}(\mathbf{x}) = \frac{1}{M} \sum_{u=-1}^1 \sum_{v=-1}^1 \sum_{w=-1}^1 \hat{v}(\mathbf{x}) \cdot \hat{v}(\mathbf{x}_x+u, \mathbf{x}_y+v, \mathbf{x}_z+w) \quad (3)$$

The LPC is based on inner products, which by definition results in sensitivity to blood-flow direction. Averaging of the velocities in the neighborhood provides built-in robustness to noise. By normalizing the velocities, as proposed by Chung et al. [3], this feature is not sensitive to the blood-flow speed.

Eigenvalue Coherence (EVC)

An alternative coherence metric was introduced by Solem et al. [12]. Instead of considering angles, they determine the coherence based on a local *distribution of orientations*. An orientation distribution is computed as the average structure tensor [4] of velocities in a local neighborhood. The structure tensor is used as the tensor product of a velocity vector with itself.

To obtain the coherence metric, eigenanalysis is performed on the average structure tensor T at each voxel

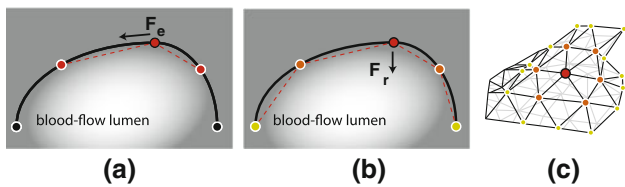


Fig. 5 Schematic overview of the internal forces [1]. **a** The elasticity force F_e operates in the tangential direction, based on the direct neighbors. **b** The rigidity force F_r operates in the normal direction, based on the second-order neighborhood. **c** For the active surface model, this approach is applied to a 3D surface, restraining excessive deformation

position. The eigenvectors span the basis of the orientation distribution. Intuitively, this can be thought of as an ellipsoid that represents the variation of orientations in the local neighborhood. When the original velocity directions are locally coherent, the ellipsoid is elongated, with a dominant principal eigenvector. However, when the original velocity directions were incoherent, the ellipsoid becomes spherical.

The coherence can, therefore, be derived from the lengths of the eigenvectors of the local structure tensor. Hence, the local eigenvalue coherence metric is defined as a ratio of the ordered eigenvalues λ_i :

$$evc(\mathbf{T}) = \left(\frac{\lambda_1 - \lambda_2}{\lambda_1 + \lambda_2} \right)^2 \tag{4}$$

Due to the tensor product, this feature is only sensitive to orientation, discarding the sign of the velocity direction. It is fair to assume that within a small blood-flow region there will be no directly opposing blood-flow directions. Therefore, orientation information is sufficient. Furthermore, EVC is sensitive to the blood-flow speed and is considerably robust to noise.

Active surface segmentation

An active surface model deforms a parametric surface, until the surface closely approximates the boundaries of interest in the provided data set. In comparison to other segmentation methods, active surfaces are computationally efficient and can operate with sub-voxel accuracy. Moreover, active surfaces are topologically stable and generally robust to noise.

However, active surface models suffer from numerical instability and may converge to local minima. The impact of these disadvantages is minimized when the model is provided with an approximate initial surface. Our approach to generate such a surface was described in section “Initial surface extraction”.

The surface is provided with a potential energy, moving the surface towards edges in the attractor image. For our application, this attractor image, or energy image, is based on the features described in section “Feature extraction”. In

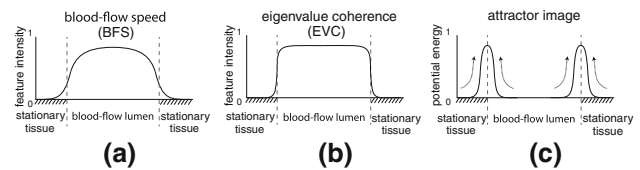


Fig. 6 Schematic overview of the external forces. **a** The intensity profile across a vessel shows a gradual slope around the boundaries for the BFS. **b** By including direction information, the EVC feature defines sharper boundaries. **c** The gradient magnitude of these features provides an attractor image, defining the potential forces (arrows)

addition, the active surface has an internal energy, determined by the surface shape.

The active surface model aims to minimize the total energy functional, which is defined as the sum of the potential energy and the internal energy. Minimizing the total energy is equivalent to solving the corresponding Euler–Lagrange equation, which is performed by means of a gradient descent approach [1]. This derivation results in a force balance between the internal forces F_{int} and the potential forces F_{pot} , defined for each node \mathbf{n} of the surface mesh as:

$$F_{int}(\mathbf{n}) = w \cdot F_{pot}(\mathbf{n}), \text{ with } F_{int} = \alpha \cdot F_e(\mathbf{n}) + \beta \cdot F_r(\mathbf{n}) \tag{5}$$

The *internal forces* restrain excessive surface deformations. On the one hand, an elasticity force F_e limits stretching of the surface. On the other hand, a rigidity force F_r restrains inordinate bending. The computation of these forces, respectively, depends on the first- and second-order surface derivatives. These derivatives are approximated numerically on the surface mesh [1], using the first- and second-order node neighborhoods, as depicted in Fig. 5a and b. The stretching and bending constraints are imposed on all nodes of the three-dimensional surface mesh (Fig. 5c), yielding smoothness of the surface.

The *external forces* attract the surface towards the boundaries between blood-flow regions and stationary tissue. The direction and strength of these potential forces F_{pot} are drawn from an attractor image, based on the features introduced in “Feature extraction”.

In Fig. 6a and b, we depict an intensity profile across a vessel of the BFS and the EVC feature, respectively. By incorporating the blood-flow direction, the EVC feature provides relatively sharp edges at the blood-flow lumen boundaries. In contrast, the BFS shows a gradual intensity change. As a result, the EVC provides a better indication of the desired boundary locations. This also holds for the LPC feature.

As opposed to the image features, the attractor image requires a maximum intensity at the desired boundaries, with a gradual intensity change towards these maxima. Therefore, we employ an elementary edge detection on the BFS and the EVC feature, using the gradient magnitude operator. The

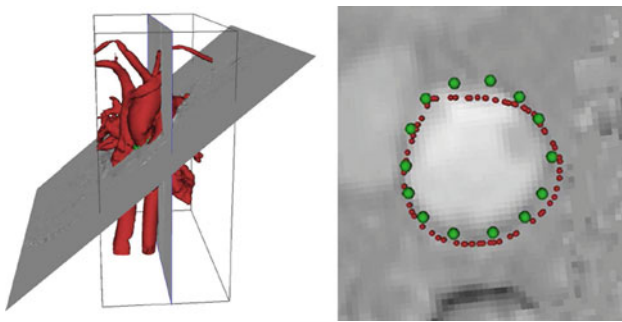


Fig. 7 (left) 3D-cine blood-flow data with segmented surface and oblique 2D-cine validation slice. (right) Manually segmented contour on 2D-cine slice (large green dots) and computed surface cross-section (small red dots)

resulting attractor image is schematically depicted by the intensity profile in Fig. 6c. By definition, the LPC feature can be applied directly as attractor image.

The potential forces are drawn from the attractor image, for each node on the surface mesh. The surface is attracted towards the boundaries, as depicted by the curved arrows in Fig. 6c. To the best of our knowledge, coherence-based features have not been employed before, to define the external forces of an active surface model.

The active surface model can be parameterized by three weighting parameters α , β , and w . With these parameters, the user can steer the force balance, where α and β increase surface smoothness and w increases influence of the blood-flow information. All parameters were scaled to a [0,1] range. The active surface model iterates until the system reaches equilibrium, or arrives at a maximum number of iterations.

Validation

For each 3D-cine PC-MRI data set, a number of 2D-cine PC-MRI slices are available. These 2D-cine slices are acquired perpendicular to the vessel of interest, measuring the through-plane flow as a scalar value (Fig. 7). Acquisition of these slices allows higher spatial and temporal resolution compared to the 3D-cine blood-flow acquisition. Therefore, the 2D-cine slices can be used as a local approximation of the ground truth.

Obtaining an approximate 3D ground-truth segmentation is difficult. Acquisition of higher resolution volumetric flow data is not feasible with current MRI sequences. Moreover, manual segmentation of the 3D luminal geometry is tedious and time-consuming, and therefore, not practicable for larger validation studies.

First, the blood-flow lumen is manually segmented using a 2D-cine slice, similar to segmentations performed in clinical practice. This results in a reference contour that captures

the blood-flow region, described by a point set in patient coordinates.

Second, the cross-section of active surface and the 2D-cine slice is determined, resulting in a point set that describes the cross-section contour (Fig. 7).

Lastly, the correspondence between the two discrete contours needs to be computed. Therefore, we have adopted a variation on the distance-to-closest-point (DCP) measure, which provides an intuitive distance in millimeters. Since the point correspondence between the two contours is not a one-to-one relation [5], point correspondences are determined bi-directionally between the two contours.

Results

The validation was performed using four volunteer studies, inspecting two 2D-cine velocity-encoded slices per study. One slice is oriented perpendicular to the aorta, and one slice is oriented perpendicular to a region of the pulmonary artery.

Table 1 provides an overview of the validation results. For each of the inspected regions, the distance between the active surface segmentation and the manually segmented reference contour is provided in millimeters. This is based on the distance-to-closest-point metric. To demonstrate the feasibility of our active surface approach, the optimal segmentation was obtained by varying the user parameters on a case-by-case basis.

The results show that the average distance between the active surface segmentation and the reference contour is generally less than 2.5 mm, which is smaller than the voxel size of the 3D-cine blood-flow data. All values larger than 2.5 mm are presented in italics in Table 1. This shows that both coherence measures provide a better attractor image for the active surface model, and hence that the blood-flow direction information is worthwhile to incorporate in the segmentation approach. Furthermore, we observe that there is no significant performance difference between both coherence measures.

A preliminary general parameter set provides acceptable segmentations, although the stringent requirement of voxel accuracy is no longer achieved. The global parameter set is derived for the LPC and the EVC feature, computing the mean parameters with their standard deviations. For the LPC metric, the parameter set becomes $(\alpha, \beta, w) = (0.05 \pm 0.03, 0.04 \pm 0.04, 0.13 \pm 0.03)$, while for the EVC metric, we propose $(\alpha, \beta, w) = (0.09 \pm 0.03, 0.05 \pm 0.02, 0.16 \pm 0.09)$. Note that all parameters are defined in a [0,1] range, and that therefore, the range of variation per parameter is considerably small.

Table 1 Validation results

#	Region-of-interest	Blood-flow speed (α, β, w)	Local phase coherence (α, β, w)	Eigenvalue coherence (α, β, w)
1	Aorta	1.80 (0.03, 0.05, 0.15)	1.55 (0.03, 0.10, 0.14)	1.29 (0.11, 0.06, 0.10)
2	Aorta	<i>3.04</i> (0.03, 0.07, 0.25)	2.07 (0.07, 0.03, 0.10)	1.78 (0.12, 0.10, 0.15)
3	Aorta	2.92 (0.07, 0.01, 0.12)	2.44 (0.02, 0.01, 0.20)	1.95 (0.07, 0.04, 0.20)
4	Aorta	2.31 (0.05, 0.03, 0.08)	2.01 (0.06, 0.03, 0.09)	1.85 (0.07, 0.04, 0.04)
1	Pulmonary artery (trunk)	3.17 (0.10, 0.10, 0.30)	1.38 (0.03, 0.10, 0.14)	1.47 (0.11, 0.06, 0.10)
2	Pulmonary artery (left)	2.78 (0.07, 0.05, 0.35)	1.81 (0.10, 0.03, 0.15)	1.88 (0.10, 0.03, 0.20)
3	Pulmonary artery (right)	2.99 (0.10, 0.02, 0.20)	1.76 (0.05, 0.03, 0.15)	1.97 (0.07, 0.04, 0.12)
4	Pulmonary artery (left)	1.97 (0.02, 0.02, 0.25)	1.64 (0.02, 0.01, 0.10)	1.52 (0.05, 0.03, 0.35)

Parameters α , β and w are unitless weights, in the range [0,1]. The average contour distance, measured using distance-to-closest-point (DCP), is defined in millimeters. Distances larger than the voxel size are italicized

Discussion

All figures presented in this work are consistently obtained from one volunteer data set. The presented segmentation approach was implemented using the C++ programming language, using the Visualization Toolkit (VTK) library [16].

Active surface models are computationally efficient, in particular when the initial surface provides a good approximation of the end result. After the initial surface is roughly determined by visual inspection, the algorithm execution time is on the order of seconds. Pre-computation of the attractor images also takes merely seconds and is required only once.

To perform the active surface segmentation, first an iso-threshold is required to extract the initial surface. In general, the iso-threshold is defined conservatively, imposing a reasonable amount of undersegmentation. This minimizes the chance that segmented structures will overlap, due to partial volume effects. For the four presented volunteers cases, the initial iso-thresholds varied between 0.3 and 0.45, in a [0,1] range. There is no need for a time-consuming search for the optimal iso-threshold.

Subsequently, the active surface segmentation is performed autonomously, based on the three user parameters. Four volunteer studies were validated, locally assessing the quality of the segmentation under varying conditions. The results show that the commonly used BFS feature performs poorly for the envisioned segmentation, in contrast to both coherence-based features.

The presented validation, based on 2D-cine PC-MRI slices, limits the regions that can be evaluated. For instance, bifurcations are difficult to assess quantitatively. However, qualitative inspection shows promising segmentations of bifurcating regions. In general, segmentation of complex morphologies is theoretically supported by the well-defined initial surface and the topological stability of the active surface.

The results of the active surface are affected by the limited spatial resolution and associated partial volume effects. Therefore, smaller arteries are challenging to segment. In addition, the active surface approach requires the blood-flow speed to be sufficiently fast to be captured by the initial threshold.

The segmentation results show that the coherence-based features provide more accurate results. In theory, these coherence measures are more reliable in turbulent blood-flow regions. Despite the large-scale turbulent behavior, the blood-flow remains locally coherent.

In this work, we have demonstrated the feasibility of an active surface segmentation of the blood-flow lumen, using the full blood-flow velocity information. In the future, a larger evaluation study may be carried out, including volunteer and patient data. This may result in a global parameter set, suitable for the majority of data sets.

Prior to such a study, it may be worthwhile to investigate automatic selection of the initial iso-threshold. Furthermore, the manual reference segmentations may be improved by including multiple expert segmentations per region.

In the future, the segmentation framework may be extended with interactive techniques to cut the surface, enabling separation of morphological structures.

Conclusions

In conclusion, we have presented an active surface segmentation approach, which facilitates meaningful quantification of blood-flow characteristics. Our approach is based on 3D-cine PC-MRI data and improves on existing techniques.

The presented approach achieves voxel accuracy under noisy conditions and deals with a substantial amount of partial volume effects. Moreover, the active surface segmentation is fast and topologically stable, given an initial approximate surface. To that end, we have presented a novel approach to

determine the initial surface, using a pre-computed tMSV volume to extract an iso-surface. This generic approach enables segmentation of complex morphology and regions with turbulent blood flow.

Our custom active surface segmentation was validated against manual segmentations, based on high-resolution 2D-cine velocity-encoded information. The reference segmentations were compared to the cross-section of the segmented surface and the slice under consideration. We show that the segmentation results closely approximate manual segmentations, in particular when a coherence measure is used to attract the surface.

Acknowledgments The volunteer 3D-cine PC-MRI blood-flow data presented in this article was provided courtesy of the division of Imaging Sciences, King's College London at St Thomas' hospital. The acquisition of 3D-cine blood-flow data was approved by the local ethics committee (KCL), and informed consent was obtained from all volunteers. In particular, we express our sincere gratitude and appreciation to professor T.Schaeffter, dr. P. Beerbaum, dr. I. Valverde, and dr. R. Clough. In addition, we would like to thank Y. Guo for her contribution to the evaluation results.

Conflict of interest None.

References

- Ahlberg J (1996) Active contours in three dimensions. PhD thesis, Linköping University
- American Heart Association (2010) Heart disease and stroke statistics. <http://www.americanheart.org/statistics>. Accessed 13 July 2011
- Chung ACS, Noble JA, Summers P (2004) Vascular segmentation of phase-contrast magnetic resonance angiograms based on statistical mixture modeling and local phase coherence. *IEEE Trans Med Imaging* 23(12):1490–1507
- Granlund GH, Knutsson H (1995) Signal Processing for Computer Vision
- Hautvast GLTF, Lobregt S, Breeuwer M, Vilanova A, Gerritsen FA (2005) Automatic contour detection in short-axis cardiac cine MR data. *J Cardiovasc Magn Reson* 7(1):323–324
- Hennemuth A, Friman O, Schumann C, Bock J, Drexler J, Huellebrand M, Markl M, Peitgen HO (2011) Fast interactive exploration of 4D MRI flow data. In: *Proceedings of SPIE*, vol 7964, pp 79640E-1–79640E-11
- Lorenson WE, Cline HE (1987) Marching cubes: a high resolution 3D surface construction algorithm. *Comput Graph Interact Tech* 21(4):163–169
- Markl M, Draney MT, Hope MD, Levin JM, Chan FP, Alley MT, Pelc NJ, Herfkens RJ (2005) Time-resolved 3-dimensional velocity mapping in the thoracic aorta: visualization of 3-directional blood flow patterns in healthy volunteers and patients. *J Comput Assist Tomogr* 28(4):459–468
- Markl M, Kilner PJ, Ebbers T (2011) Comprehensive 4D velocity mapping of the heart and great vessels by cardiovascular magnetic resonance. *J Cardiovasc Magn Reson* 13(7):1–22
- Nguyen TQH (2010) Automated blood-flow segmentation in large thoracic arteries using 4D MRI flow measurements. MSc thesis, Eindhoven University of Technology
- Persson M, Solem JE, Markenroth K, Svensson J, Heyden A (2005) Phase contrast MRI segmentation using velocity and intensity. *Scale Space PDE Methods Comput Vis* 3459:119–130
- Solem JE, Persson M, Heyden A (2004) Velocity based segmentation in phase-contrast MRI images. *Med Image Comput Comput Assist Interv (MICCAI)* 3216:459–466
- Uribe S, Tangchaoren T, Parish V, Wolf I, Razavi R, Greil G, Schaeffter T (2008) Volumetric cardiac quantification by using 3D dual-phase whole-heart MR imaging. *Radiology* 248(2):606–614
- van Assen HC, Danilouchkine MG, Dirksen MS, Reiber JHC, Lelieveldt BPF (2008) A 3D active shape model driven by fuzzy inference: application to cardiac CT and MR. *IEEE Trans Inf Technol Biomed* 12(5):595–605
- van Pelt R, Bescòs JO, Breeuwer M, Clough RE, Gröller ME, ter Haar Romeny B, Vilanova A (2010) Exploration of 4D MRI blood flow using stylistic visualization. *IEEE Trans Vis Comput Graph* 16(4):1339–1347
- The Visualization Toolkit. <http://vtk.org>. Accessed 13 July 2011